HHS Public Access

Author manuscript

ACS Appl Mater Interfaces. Author manuscript; available in PMC 2021 February 19.

Published in final edited form as:

ACS Appl Mater Interfaces. 2020 February 19; 12(7): 7869–7878. doi:10.1021/acsami.9b16867.

A New Strategy for Reporting Specific Protein Binding Events at Aqueous-Liquid Crystal Interfaces in the Presence of Non-Specific Proteins

Chul Soon Park[1,†], **Kazuki Iwabata**[1,†], **Uma Sridhar**[3,†], **Michael Tsuei**[2,†], **Khushboo Singh**[3], **Young-ki Kim**[2,4], **S. Thayumanavan**[3,*], **Nicholas L. Abbott**[2,*]

[1]Department of Chemical and Biological Engineering, University of Wisconsin-Madison, Madison, WI 53706, USA

[2]Smith School of Chemical and Biomolecular Engineering, Cornell University, Ithaca, NY 14853, USA

[3]Department of Chemistry, University of Massachusetts Amherst, Amherst, MA 01003, USA

[4]Department of Chemical Engineering, Pohang University of Science and Technology, Pohang, Gyeongbuk 37673, Korea

Abstract

Aqueous-liquid crystal (LC) interfaces offer promise as responsive interfaces at which biomolecular recognition events can be amplified into macroscopic signals. However, the design of LC interfaces that distinguish between specific and non-specific protein interactions remains an unresolved challenge. Herein we report the synthesis of amphiphilic monomers, dimers and trimers conjugated to sulfonamide ligands via triazole rings, their assembly at aqueous-LC interfaces, and the orientational response of LCs to the interactions of carbonic anhydrase II (CAII) and serum albumin with the oligomer-decorated LC interfaces. Of six oligomers synthesized, only dimers without amide methylation were found to assemble at aqueous interfaces of nematic 4-cyano-4'-pentylbiphenyl (5CB) to induce perpendicular LC orientations. At dimer-decorated LC interfaces, we found that concentrations of CAII less than 4 μM did not measurably perturb the LC but prevented non-specific adsorption and penetration of serum albumin into the dimer-decorated interface that otherwise triggered bright, globular LC optical domains. These experiments and others (including competitive adsorption of CAII, BSA and lysozyme) support

[*]**Corresponding Author:** thai@chem.umass.edu, nabbott@cornell.edu.
[†]These authors contributed equally to this work.

Supporting Information

Synthetic pathways, procedures and characterization of oligomers (Figures S1–S4); Optical images of LC interfaces decorated with methylated and non-methylated monomers, dimers, and trimers (Figure S5); Kinetics of oligomer desorption from LC interfaces (Figure S6); Confocal fluorescence micrographs of high concentrations of CAII adsorbed at oligomer-decorated LC interface (Figure S7); CAII concentration-dependence of LC anchoring (Figure S8); Optical intensities of LC interfaces as a function of time with high concentrations of sulfonamide inhibitors (Figure S9); Optical micrographs of LC films decorated with CAII and BSA exposed to different concentrations of thermolysin (Figure S10).

CONFLICT OF INTEREST

Nicholas Abbott has a financial interest in Platypus Technologies LLC, a company that has commercialized liquid crystal-based analytical technology

The authors declare no competing financial interest

our hypothesis that specific binding of CAII to the dimer prevents LC anchoring transitions triggered by non-specific adsorption of serum albumin. We illustrate the utility of the approach by reporting (i) the relative activity of two small molecule inhibitors (6-ethoxy-2-benzothiazolesulfonamide and benzenesulfonamide) of binding of CAII to sulfonamide, and (ii) proteolytic digestion of a protein (CAII) by thermolysin. Overall, the results in this paper provide new insight into the interactions of proteins at aqueous-LC interfaces and fresh ideas for either blocking non-specific interactions of proteins at surfaces or reporting specific binding events at LC interfaces in the presence of non-specific proteins.

Keywords

liquid crystal; specific binding; proteins; non-specific; oligomers; inhibitors

1. INTRODUCTION

Protein-ligand binding at interfaces is important in a range of fundamental and applied contexts, including cell signaling pathways[1–3], diagnostic assays for use in low-resource environments[4–5], and drug discovery[6–7]. Accordingly, a variety of techniques have been developed to measure specific protein-ligand binding events, including surface plasmon resonance (SPR)[8], fluorescence resonance energy transfer (FRET)[9], fluorescence[10], transient-induced molecular electronic spectroscopy[11], and small-molecule microarrays[12]. The most successful of these techniques achieve specificity towards a targeted protein by combining molecular recognition with a method of amplification/transduction that incorporates some level of additional specificity (e.g., the use of enzymes for amplification)[7]. These techniques, however, are often less than optimal for reporting protein-ligand binding events in low-cost or high throughput assays, due to the need for either complex instrumentation (e.g., SPR[8]) or multiple labeling/binding steps[9] (typically involving fluorescently labelled reporter molecules).

Past studies have revealed that the long-range ordering and surface sensitivity of liquid crystals (LCs) can be used to amplify the presence of a range of chemical (e.g., glucose[13–14] and heavy metals[15–16]) and biological species (lipids[17–20], proteins[19, 21–27] and DNA[28–29], and mammalian[30] and bacterial[31] cells) at interfaces into optical signals. Of relevance to the study reported in this paper, interfaces formed between thermotropic LCs and aqueous phases[19, 32–34] are particularly promising for reporting interactions involving biological species because (i) they do not require the use of labels (e.g., fluorescent) to detect biomolecular binding events, (ii) LC interfaces are mobile, and thus permit lateral reorganization of species in ways that mimic biomolecular interactions at cell membranes, and (iii) the experimental set-up is relatively simple and thus potentially applicable to the development of diagnostics for use in low-resource environments[17, 35–38]. An additional useful attribute of a LC-based amplification/transduction approach is that the response of the LC is dependent on the structure of the adsorbate[28, 32, 34], thus providing a second level of specificity in the response (beyond that provided by a molecular recognition step). For example, surface active species such as surfactants and lipids produce responses in LCs that are distinct from non-specific protein adsorption[38–41].

While the studies described above serve to illustrate the promise of aqueous-LC interfaces for reporting biological phenomena, there exist a range of unresolved issues that need to be addressed to realize the full potential of LC technology in the context of biomolecular analytics[42]. Specifically, general and robust approaches that permit detection of specific protein binding events in the presence of non-specific proteins remain to be developed[17, 24, 35–38, 43]. For example, at aqueous-LC interfaces decorated with phospholipids, both proteins and peptides have been reported to penetrate into the phospholipid monolayers, driving the reorganization of the monolayers and generating an optical response (domains) in the LCs[19, 39, 44]. Past studies have demonstrated a strong correlation between the shapes (fractal dimensions) of the micrometer-scale optical domains on the LC interface and the secondary structures of adsorbed proteins and peptides[19, 39–40, 44].

Motivated by the challenge of sensing specific protein binding events at LC interfaces in the presence of proteins that bind non-specifically, herein we report a study of the binding of carbonic anhydrase II (CAII) to sulfonamide-functionalized oligomers[45] in the presence of serum albumin. The amphiphilic oligomers (Figure 1) were designed and synthesized to incorporate three functional groups – (i) alkyl chains that penetrate into the LC and influence its ordering[34, 46], (ii) oligoethylene glycol groups that minimize non-specific interactions with proteins[24, 37–38], and (iii) sulfonamide moieties that specifically bind to the target protein, CAII[47–48]. These oligomers (monomers, dimers, trimers) were synthesized in a modular fashion through the use of triazole rings as sites for conjugation of sulfonamide functional groups[46, 49–50].

A key result emerging from our study is that specific binding of CAII to sulfonamide-functionalized dimers prevents LCs from responding to non-specific interactions of serum albumin proteins. We show how this finding can be exploited to form the basis of a new strategy for measuring specific binding interactions. Furthermore, we illustrate the utility of the strategy by detecting small molecule inhibitors (i.e. ethoxzolamide and benzenesulfonamide) of CAII and we show how the observation can be used to report the activity of a protease (i.e. thermolysin)[47–48]. Overall, the results presented in this paper provide a first step towards development of a new strategy that enables the use of LCs for reporting specific binding events and the activity of enzymes in the presence of proteins that bind non-specifically.

2. MATERIALS AND METHODS

Materials.

The nematic LC 4-cyano-4’-pentylbiphenyl (5CB), manufactured by BDH, was purchased from EM Industries (Hawthorne, NY). Phosphate buffer saline (PBS), bovine serum albumin (BSA), lysozyme from chicken egg white, carbonic anhydrase II, 6-ethoxy-2-benzothiazolesulfonamide (ethox), and benzenesulfonamide were obtained from Sigma-Aldrich (Milwaukee, WI). Dimethyloctadecyl-[3-(trimethoxylsilyl)propyl]-ammonium chloride (DMOAP) was obtained from Acros Organics. Glass microscope slides were Fisher’s Finest Premium Grade obtained from Fisher (Pittsburgh, PA). Gold-coated transmission electron microscopy (TEM) grids (18 μm in thickness, 280 μm in grid spacing

and 60 μm bar width) were obtained from Electron Microscopy Sciences (Fort Washington, PA). The synthetic procedures used to prepare the oligomers used in our study (***H***-monomer, ***H***-dimer, ***H***-trimer, ***CH$_3$***-monomer, ***CH$_3$***-dimer, and ***CH$_3$***-trimer, Figure 1) are provided in the Supporting Information (See Scheme S1 to S4).

Synthesis of Oligomers.

We illustrate our approach for synthesis of the oligomers employed in this study by using the ***H***-dimer as an example. ***H***-dimer (Scheme 1) was synthesized via a 12-step synthetic protocol from 3,5 dihydroxy benzoic acid. **8** was synthesized via reaction of **5** with ethylenediamine in dry DCM, TEA with a yield of 72%. **12** was synthesized via reaction of p-carboxy benzenesulfonamide with N-hydroxysuccinimmide in anhydrous tetrahydrofuran. Synthesis of the sulfonamide ligand (**16**) involved reacting **12** and **15** in anhydrous tetrahydrofuran and triethylamine. **8** and **16** were used in a copper-catalyzed click reaction in anhydrous tetrahydrofuran and triethylamine to produce the ***H***-dimer in 72% yield. Following concentration of the ***H***–dimer product mixture in vacuum, the product was dissolved in water and extracted with ethyl acetate. Characterization of ***H***-dimer using ^{1}H NMR showed the disappearance of a peak corresponding to the propargyl group at 3.08 ppm and the presence of a peak at 7.61 ppm corresponding to the triazole proton, indicating successful alkyne-azide click reaction. All oligomers and reactants used in Scheme 1 were characterized via ^{1}H NMR, ^{13}C NMR, and ESI-MS.

Preparation of DMOAP-modified Glass Slides.

A 1% v/v DMOAP solution used to modify the glass slides was prepared by adding 1.4 mL 60% v/v DMOAP (in methanol) into 140 mL Milli-Q water. Glass microscope slides free of dust and other visible imperfections were then immersed in the 1% v/v DMOAP solution and placed into a sonicating bath for 10 minutes at room temperature. Following sonication, the glass slides were removed from the 1% v/v DMOAP solution and subsequently rinsed with Milli-Q water followed by ethanol to remove unreacted DMOAP from the surfaces of the slides. The DMOAP-coated glass slides were then dried under a stream of nitrogen gas. The quality of the DMOAP monolayer formed on the surface of the glass slides was tested by first pairing two DMOAP-treated glass slides, using ~15 μm-thick Saran wrap as a spacer. 5CB was introduced between the slides and the resulting optical texture was observed between crossed-polarizers to confirm perpendicular alignment of LCs with respect to the LC-solid interface (homeotropic anchoring). Any sample not exhibiting a dark optical texture indicative of homeotropic anchoring was not used in subsequent experiments[51].

Preparation of Amphiphilic Oligomer and Inhibitor Solutions.

Amphiphilic oligomer was dissolved in acetone to produce a stock solution with a concentration of 10 mg/mL. An aliquot of the stock solution was transferred to a new glass vial and dried for an hour under vacuum at room temperature. After measuring the weight of the vial containing the dried oligomer, a small volume of acetone (final composition 2% v/v acetone) was added to the vial to dissolve the oligomer and 10 mM PBS was added to achieve the target concentration. For the ***H***-dimer, the final concentration was 20 μM. The solution was stirred for approximately 16 hours at room temperature to remove acetone from

the solution. Following the 16 hour incubation, a small population of ***H***-dimer aggregates were observed in the PBS. Prior to use, the solutions were sonicated for 30 sec to disperse the aggregates. Aqueous solutions containing 100 μM ethox in PBS were prepared using the same procedure that was used to prepare the dispersion of ***H***-dimer. Benzenesulfonamide was directly dissolved in PBS to a final concentration of 2 mM.

Preparation of Aqueous-LC Interface.

Gold-coated TEM grids were cleaned sequentially with acetone and ethanol, and then dried. The grids were then placed onto the surfaces of DMOAP treated glass slides. 0.5 μL of 5CB was dispensed onto each grid and the excess 5CB was removed using a micro syringe. This procedure led to the formation of a stable film of 5CB within each specimen grid. The gold-coated grid filled with 5CB was then immersed into aqueous PBS and the 5CB film in contact with the aqueous phase was examined by optical microscopy (crossed-polarizers)[19].

Response of LC Decorated with Amphiphilic Sulfonamide Oligomers to Proteins Dissolved in PBS.

Amphiphilic oligomers were assembled at the interfaces of nematic 5CB by incubating aqueous solutions of oligomers at 30 °C against the LC interface for 15 hours. We note that at T= 30 °C, the LC films reached their steady-state orientations more quickly as compared to experiments conducted at T= 25 °C The aqueous solutions containing the amphiphilic oligomers were then replaced by 10 mM PBS. Subsequently, a stock protein solution was added to the PBS to obtain the desired protein concentration. The protein solution was incubated against the LC at 30 °C, using a heated stage to maintain the temperature while observing the sample under a polarized light microscope. For experiments involving competitive binding of proteins, 0.4 μM CAII was introduced into the aqueous phase and incubated for 60 min at 30 °C. Subsequently, a mixture of BSA and inhibitor was added to the system and the response of the LC recorded as a function of time. Quantification of the optical intensity of images was performed with NIH ImageJ software.

Response of Sulfonamide Oligomer-Decorated LC Interface to Mixtures of Thermolysin, CAII, and BSA.

A 1 mg/mL (27.6 μM) thermolysin stock solution was prepared in 10 mM PBS. The stock solution of thermolysin was diluted with PBS to a concentration of 276 pM. Additionally, solutions containing 50 μM CAII and 50 μM BSA in PBS were prepared using the same method as described above for thermolysin. A PBS aqueous solution with 0.5 mM $CaCl_2$ was also prepared for subsequent BSA digestion experiments by thermolysin. 4.3 μL of the 276 pM thermolysin solution was added into a 2 mL Eppendorf centrifuge tube that contained 562.1 μL of buffer solution (PBS and 0.5 mM $CaCl_2$). Subsequently, 9.6 μL of 50 μM CAII was added and the mixture was incubated in an oven at 65 °C for 1 hour. After an hour, the mixture was transferred to an ice bath and then 24 μL of 50 μM BSA was added into the mixture containing thermolysin, CAII, and PBS buffer with 0.5 mM $CaCl_2$. The concentration of thermolysin was ~2 pM. 375 μL of the aqueous solution in the well containing the LC decorated with amphiphilic sulfonamide oligomers was removed and replaced with 375 μL of the solution containing thermolysin + CAII + PBS buffer with 0.5

mM $CaCl_2$. The well containing 1 pM thermolysin, 0.4 μM CAII, and 1 μM BSA in PBS was then incubated for 1 hour prior to imaging.

3. RESULTS AND DISCUSSION

Design and Synthesis of Sulfonamide-Functionalized Oligomers.

At the outset of this study, we designed and synthesized six amphiphilic oligomers (Figure 1). The oligomers are modular and comprise three design motifs; alkyl chains, oligoethylene glycol, and sulfonamide moieties incorporated via triazole rings. Each motif was introduced to achieve a specific function. First, the alkyl chains were used to anchor the amphiphilic oligomers at the LC interface. The number of alkyl chains presented by the amphiphilic oligomers strongly influences their stability (reversibility of adsorption) at the aqueous-LC interface[34, 46]. Second, oligoethylene glycol moieties were introduced as hydrophilic spacers to minimize non-specific/electrostatic interactions with proteins and promote solubility of the oligomers in the aqueous phase[52–54]. Past studies have reported that polyethylene glycol (PEG)-decorated interfaces exhibit low levels of non-specific adsorption of proteins relative to those observed at charged or hydrophobic surfaces[52–54]. At aqueous-LC interfaces, PEGylated mesogens have been shown to minimize non-specific adsorption of proteins[24]. Third, the sulfonamide moiety was introduced into oligomers to specifically bind CAII, as described in a previous study by Gao *et al.*45 The synthetic strategy, however, has been demonstrated to allow the introduction of binding groups for proteins other than CAII into the oligomers (e.g., biotin for avidin and 2,4-dinitrophenol for anti-2,4-dinitrophenol antibodies, see SI for details).

The six oligomers synthesized were named according to whether or not amide groups present in the molecules were methylated (R_1=H; R_2=CH_3). The amphiphilic oligomers without methylated amide groups can participate in hydrogen-bonding in ways that are not possible for the methylated oligomers[55]. Consistent with this proposition, the critical aggregation concentrations (CAC) of methylated oligomers are higher than non-methylated oligomers (Figures S1 to S4). Additionally, Raghupathi *et al.* reported that the presence of amide bonds induces intramolecular hydrogen-bonding and conformational rigidity of the backbone[50]. This leads to amphiphilic supramolecular assemblies that exhibit temperature-dependent organizations[50].

LC Anchoring Transitions at Aqueous Interfaces Decorated with Amphiphilic Oligomers.

Our initial experiments explored the effects of oligomer (Figure 1) assembly at aqueous-LC interfaces on the ordering of nematic LCs (5CB). In these experiments, LCs were hosted in the pores of TEM grids supported on glass microscope slides that were functionalized with DMOAP[51]. The DMOAP treatment causes perpendicular alignment (homeotropic anchoring) of LCs at this interface (see Materials and Methods for details). Immersion of LC-filled specimen grids into aqueous PBS resulted in tangential alignment (planar anchoring) of LCs at their aqueous-LC interfaces (Figure 2a,b). Figure 2a shows an optical micrograph of a LC film captured using crossed-polarizers (transmission mode).

Past studies have shown that adsorption of proteins at aqueous-LC interfaces typically induces planar anchoring of LCs[56–57]. Informed by these observations, our initial studies of the assembly of oligomers at LC interfaces centered on whether the oligomers would promote homeotropic anchoring of the LCs. With homeotropic anchoring as the initial state, guided by the results of past studies[19, 40–41], we hypothesized that protein binding would be reported via a change from homeotropic to planar LC anchoring. Interestingly, we found that the ***H***-dimer (Figure 1b) was the only oligomer of the six studied to induce homeotropic anchoring upon assembly at aqueous (PBS)-LC interfaces (Figure 2c,d, Figure S5). The ***H***-dimer-decorated LC interfaces were found to maintain their homeotropic orientation upon subsequent exchange of the aqueous phase with PBS free of ***H***-dimer (Figure S6). A complete set of optical micrographs obtained using each of the six synthesized oligomers is presented in Figure S5. We note that LC responses were measured below and above CACs of the oligomers, and the ***H***-dimer only caused homeotropic anchoring. We do not yet fully understand why only the ***H***-dimer causes homeotropic anchoring of LCs; ongoing studies are addressing this question. Below we focus on an investigation of the interactions of proteins (specific and non-specific) with interfaces of LCs decorated with the ***H***-dimer.

Protein Binding Events at Aqueous-LC Interfaces Decorated with the *H*-Dimer.

Next, we investigated how nematic 5CB interfaces decorated with ***H***-dimer responded to binding events involving CAII[58–61] (Figure 3a,d,S7), bovine serum albumin (BSA, Figure 3b,e) and lysozyme (Figure 3c,f). Prior to addition of the proteins, the aqueous solution of ***H***-dimer was exchanged with PBS. As shown in Figure 3a, addition of 0.4 μM CAII results in a dark optical appearance indicative of homeotropic LC anchoring. Evidence of specific binding of CAII to sulfonamide at the LC interface is presented below (via introduction of different inhibitors of CAII binding).

Next, we contacted ***H***-dimer-decorated LC interfaces with 4 μM BSA (Figure 3b) and observed the optical appearance of the LC films to change from dark to bright over the course of an hour. A similar response to that observed in Figure 3b was also recorded when the concentration of BSA was 1 μM. Visual inspection of the progression of interference colors of the LC films indicated formation of a tilted LC orientation. This observation suggests non-specific binding of BSA to the ***H***-dimer decorated LC interface (Figure 3e). The result differs from prior observations of Brake *et al.*[19], where D-α-dipalmitoyl phosphatidylcholine (D-DPPC)-laden aqueous-LC interfaces did not respond to the addition of 1–10 μM BSA, suggesting that D-DPPC is more resistant to non-specific adsorption of BSA than the ***H***-dimer. Interestingly, incubation of 4 μM lysozyme against the dimer decorated aqueous-LC interface for 16.5 hours did not perturb the LC from the initial homeotropic anchoring (Figure 3c,f).

To understand the possible origins of the difference in LC response to the presence of either BSA or lysozyme, we considered the physical properties of the two proteins (Table 1). The isoelectric points of the proteins indicate that the net charges of BSA and lysozyme under our experimental conditions (PBS, pH 7.4) are negative and positive, respectively. We also measured the zeta-potentials of LC droplets in water, PBS, and 20 μM ***H***-dimer (Table 2). These measurements revealed that the zeta potentials are negative under all conditions

investigated, and thus that interactions between the LC interfaces and proteins involving net charge would be attractive for lysozyme and repulsive for BSA (in contradiction to our experimental observations involving the response of the LC). However, past studies have revealed that the spatial distribution of charge over the surfaces of proteins (not just net charge) plays a key role in mediating protein interactions with interfaces[62–63], and that other colloidal forces (e.g., hydrophobic[64–65]) are also typically important. BSA, in particular, binds hydrophobic substrates strongly[65–67], and we speculate that hydrophobic interactions rather than charge interactions dominate the relative responses of the LC to BSA and lysozyme.

Specific Binding of CA II to Sulfonamide Blocks Response of LC to Non-Specific Proteins.

Inspired by our observations that ***H***-dimer-decorated LC interfaces changed orientation upon binding of BSA but not of CAII, next we explored the consequences of sequential binding of specific and non-specific proteins. First we incubated the LC against a 20 μM ***H***-dimer solution for one hour. Next, 0.4 μM CAII was introduced into the aqueous bulk and equilibrated for two hours. 1 μM BSA was then added and equilibrated for an additional two hours (Figure 4a,e). Inspection of Figure 4a,e reveals that, following equilibration with BSA, the LC film maintains homeotropic anchoring. This observation contrasts with results of the type shown in Figure 3b and led us to hypothesize that binding of CAII to the sulfonamide moiety at the LC interface blocked non-specific binding of BSA. We also performed an experiment in which 0.4 μM CAII and 1 μM BSA were introduced simultaneously into the aqueous bulk (Figure 4b,f). Inspection of the LC interface following a two hour incubation revealed that the LC interface maintained homeotropic anchoring. This result suggests that CAII binds to the sulfonamide moiety at the LC interface faster than BSA, thus blocking non-specific binding of BSA with the aqueous-LC interface. Although we explore further this result below in the context of reporting specific protein binding events at LC interfaces in the presence of non-specific proteins, we note here that the result also hints at a strategy for blocking non-specific interactions of proteins at surfaces.

Additionally, we introduced 1 μM lysozyme and 1 μM BSA into an aqueous bulk in contact with a ***H***-dimer-decorated LC interface either sequentially (Figure 4c,g) or simultaneously (Figure 4d,h) and allowed the system to equilibrate for two hours. In both cases, the LC-interface responded to the addition of BSA, showing a bright optical texture indicative of tilted anchoring (Figure 4c,d). These results support our hypothesis that lysozyme does not bind to LC interfaces decorated with ***H***-dimers with sufficient strength to block BSA adsorption.

Motivated by our proposal that binding of CAII to ***H***-dimer-decorated LC interfaces blocks non-specific binding of BSA, we explored the influence of CAII concentration on the LC response to BSA. We prepared solutions of 1 μM BSA containing either 0.1, 0.2, 0.3 or 0.4 μM of CAII. These protein mixtures were equilibrated against ***H***-dimer-decorated LC interfaces (Figure S8). For ***H***-dimer-decorated LC interfaces equilibrated against 0.1 μM CAII and 1 μM BSA, a transition from homeotropic to tilted anchoring was observed. For ***H***-dimer-decorated LC interfaces equilibrated against 0.4 μM CAII and 1 μM BSA, however, the LC film remained homeotropic, indicating that BSA did not bind to the

aqueous-LC interface to an extent that an anchoring transition was triggered. As detailed in Figure S8, the intermediate concentrations of CAII led to responses in the LC that were intermediate to those reported above when using 0.1 and 0.4 μM CAII. Overall, these results reveal that the concentration of CAII in the aqueous bulk influenced the LC response to non-specific binding of BSA. Furthermore, these observations are in general agreement with the magnitude of the dissociation constant (K_d) between CAII and benzenesulfonamide (K_d=970 nM[68]). Guided by this result, we used 0.4 μM CAII in our subsequent investigations detailed below.

Detection of Specific Binding between CAII and Sulfonamide using Inhibitors.

The results described above support our proposal that the ***H***-dimer-decorated interface of the LC can report specific binding events involving CAII in the presence of non-specific proteins such as BSA. In this section, we demonstrate the utility of this finding by showing that it is possible to report the activity of two small-molecule inhibitors of CAII (ethoxzolamide (Figure 5a) and benzenesulfonamide (Figure 5b)). Ethoxzolamide (ethox) has a dissociation constant (K_D) of 0.1 nM[68]. In our experiments, 0.4 μM CAII was introduced into the aqueous bulk and incubated against the ***H***-dimer-decorated LC interface for two hours. Next, a mixture of 1 μM BSA with or without 4 μM ethox was added to the aqueous bulk. When the ***H***-dimer-CAII-decorated aqueous-LC interface was exposed to BSA and inhibitor, the optical appearance of the LC film transitioned from dark to bright, indicative of non-specific binding of BSA to the aqueous-LC interface (Figure 5c).

Examination of the kinetics of the LC response revealed the brightness of the aqueous-LC interface to increase monotonically with time (red circles, Figure 5g). In contrast, when 1 μM BSA was added without inhibitor a near-baseline response was observed (blue squares, Figure 5g). Additionally, responses of ***H***-dimer-decorated LC interfaces free of CAII (green triangles, Figure 5g) showed similar responses to samples containing CAII, BSA and ethox. This result suggests that ethox competitively displaces CAII binding to the ***H***-dimer at the LC interface. Following dissociation of CAII from the ***H***-dimer-decorated LC interface, BSA non-specifically binds to the LC interface, thereby triggering the observed LC transition away from the homeotropic orientation (Figure 5c,g).

Next, we investigated the effect of inhibitor binding affinity on the LC response by replacing ethox (K_D = 0.1 nM) with benzenesulfonamide (K_D = 970 nM[68], Figure 5b). In the presence of benzenesulfonamide (4 μM), BSA and CAII, the LC film maintained homeotropic anchoring after equilibration for two hours (Figure 5d). This result suggests that the addition of 4 μM benzenesulfonamide did not inhibit binding of CAII to the ***H***-dimer (Figure 5h). Upon increasing the concentration to 40 μM, we observed an optical response corresponding to ~30% of that of samples containing BSA and benzenesulfonamide in the absence of CAII (Figure S9). Overall, these observations indicate that the optical response of LC films can be used to determine binding affinities between enzymes and their inhibitors. We note that quantification of binding affinity at interfaces is complex, reflecting a range of factors including effective local concentrations and steric interactions.

Detection of Thermolysin Activity.

The results described above suggest that our system enables detection of analytes (e.g. enzyme inhibitors) that prevent CAII from binding to ***H***-dimer-decorated interfaces. Guided by these observations, we hypothesized that enzymatic digestion of CAII by a proteinase should also lead to a measurable LC response using the strategy reported in this paper. To verify this hypothesis, we used thermolysin (TLN), a well-known and thermostable metalloproteinase[69] in the experiments described below (Figure 6a,b).

First, we investigated the effect of TLN on non-specific adsorption of BSA and digested BSA fragments at aqueous-LC interfaces. Our analysis of the effects of TLN were aided by two control experiments: ***H***-dimer-decorated LC films were equilibrated with aqueous solutions of either 1 μM BSA or a mixture of both 0.4 μM CAII and 1 μM BSA for 1 hour and the optical appearance of the films 1 hour post addition of proteins was recorded. We defined the optical intensity of the LC equilibrated with 1 μM BSA to be 100% and we defined the optical response the LC equilibrated with a mixture of 0.4 μM CAII and 1 μM BSA to be 0%. Next, we incubated mixtures of 1 μM BSA with either 0.1 pM, 0.5 pM, or 1 pM TLN at 65 °C for an hour and then equilibrated the mixtures against a ***H***-dimer-decorated aqueous-LC interface. As shown in Figure 6a, the addition of TLN to the BSA resulted in no significant change in the transmission of light through the LC film (relative to samples not containing TLN). Corresponding micrographs are provided in Figure S10. These results suggest that BSA and digested BSA fragments non-specifically adsorbed to the aqueous-LC interface[70].

Second, we investigated the effect of TLN on LC films equilibrated against CAII and BSA. First, an aqueous solution containing 0.4 μM CAII and either 0.1 pM, 0.5 pM, or 1 pM TLN was incubated at 65 °C for one hour. Following the incubation period, the sample was cooled on ice to quench the activity of TLN. 1 μM BSA was subsequently added to each sample and the aqueous mixture of CAII, TLN, and BSA was equilibrated against a ***H***-dimer-decorated LC interface. As shown in Figure 6b, the optical signal from the ***H***-dimer-decorated LC interface treated with the sample to which 1 pM TLN was added is indistinguishable from the ***H***-dimer-decorated LC films in contact with aqueous BSA only (no TLN or CAII). Upon decreasing the concentration of TLN used to pretreat the CAII below 0.5 pM TLN, the LC optical signal decreased to a level generated by a sample containing 0.4 μM CAII and 1 μM BSA (Figure 6a). These results suggest that the activity of 1 pM TLN is sufficient to digest CAII molecules in the samples such that there is an insufficient number of molecules remaining in the sample that can bind to and block the ***H***-dimer-decorated interface, thereby allowing BSA to non-specifically bind to the LC interface and induce a homeotropic to planar LC anchoring transition.

The concentration dependence of TLN activity inferred from the experiment above was verified using Western blots (Figure 6b inset). Band intensities corresponding to CAII were extracted using ImageJ and subsequently converted into a normalized band intensity (calculated by dividing band intensity at a given concentration of TLN by band intensity in the absence of TLN). Differences in band intensities for TLN concentrations between 0.1 pM and 10 pM are shown in Table 3.

4. CONCLUSIONS

The results in this paper reveal that specific binding of a protein at a LC interface can prevent non-specific proteins from generating a response in the LC, which hints at several potential applications. First, it suggests that specific binding of proteins to interfaces may offer the basis of a strategy for preventing non-specific fouling of surfaces with proteins. Second, and as explored in more detail in this paper, the result suggests the basis of a new strategy for reporting specific protein binding events at aqueous-LC interfaces in the presence of non-specific proteins. We found that specific binding of CAII to sulfonamide presented by a dimeric amphiphile at an aqueous-LC interface can be transduced optically by challenging the LC interface with BSA, a protein that non-specifically binds to the LC interface. The presence of CAII specifically bound to the ***H***-dimer pre-adsorbed at the LC interfaces blocked adsorption and penetration of BSA into the dimer-decorated LC interfaces. We also demonstrated the utility of this new finding, by showing how it can be adapted to report binding of small molecule inhibitors to proteins, and the enzymatic digestion of a protein.

While our studies serve to illustrate the promise of aqueous-LC interfaces for reporting specific protein binding interactions in the presence of proteins that non-specifically bind, the work also generates a number of questions for future investigation. First, we reported a family of six oligomeric amphiphiles, but found that only one of the six caused nematic LCs to assume homeotropic anchoring. In particular, we found that the dimer containing methylated amides caused the LCs to assume planar anchoring whereas the dimer containing amide without methylation (***H***-dimer) assembled on the aqueous-LC interface to induce homeotropic anchoring. These results highlight the need for additional structure-property studies to link the molecular structure of this class of amphiphiles to their self-assembly at aqueous-LC interfaces and orient LCs. Second, we note that the strategy demonstrated in this paper, while promising, is demonstrated using CAII, dimers containing sulfonamide and BSA. Additional studies are needed to evaluate the approach using other ligand-protein interactions and proteins that can non-specifically bind to substrates. We note, however, that serum albumins are present in many biological samples (or could be added if absent) suggesting that the approach has the potential to be broadly useful. Additionally, serum samples can potentially be diluted to bring the concentration of albumins into the range that enables the strategy reported in this paper. Finally, we note that the presence of adsorbates that interfere with the binding of CAII to dimers containing sulfonamide would potentially produce false negatives. The extent to which this is a limitation to the approach reported in this paper is unknown and requires further investigation. Overall, the results reported in this paper provide initial evidence for a new approach that may find use in both fundamental studies of protein-ligand binding events and applied contexts such low-cost diagnostics.

Supplementary Material

Refer to Web version on PubMed Central for supplementary material.

ACKNOWLEDGMENT

We acknowledge support of this research from the Army Research Office through W911NF-15-1-0568 and W911NF-17-1-0575. Additional support was provided by National Science Foundation (CBET 1508987, DMR-1710318 and DMR-143595) and the NIGMS of the National Institutes of Health (GM-065255 and T32GM108556). This work made use of the Cornell Center for Materials Research Shared Facilities which are supported through the NSF MRSEC program (DMR-1719875).

REFERENCES

1. Fortanet JG; Chen CHT; Chen YNP; Chen ZL; Deng Z; Firestone B; Fekkes P; Fodor M; Fortin PD; Fridrich C; Grunenfelder D; Ho S; Kang ZB; Karki R; Kato M; Keen N; LaBonte LR; Larrow J; Lenoir F; Liu G; Liu SM; Lombardo F; Majumdar D; Meyer MJ; Palermo M; Perez L; Pu MY; Ramsey T; Sellers WR; Shultz MD; Stams T; Towler C; Wang P; Williams SL; Zhang JH; LaMarche MJ, Allosteric Inhibition of SHP2: Identification of a Potent, Selective, and Orally Efficacious Phosphatase Inhibitor. J Med Chem 2016, 59 (17), 7773–7782. [PubMed: 27347692]
2. Kopan R; Ilagan MXG, The Canonical Notch Signaling Pathway: Unfolding the Activation Mechanism. Cell 2009, 137 (2), 216–233. [PubMed: 19379690]
3. Grandy D; Shan JF; Zhang XX; Rao S; Akunuru S; Li HY; Zhang YH; Alpatov I; Zhang XA; Lang RA; Shi DL; Zheng JJ, Discovery and Characterization of a Small Molecule Inhibitor of the PDZ Domain of Dishevelled. J Biol Chem 2009, 284 (24), 16256–16263. [PubMed: 19383605]
4. Funes-Huacca M; Wu A; Szepesvari E; Rajendran P; Kwan-Wong N; Razgulin A; Shen Y; Kagira J; Campbell R; Derda R, Portable Self-contained Cultures for Phage and Bacteria Made of Paper and Tape. Lab Chip 2012, 12 (21), 4269–4278. [PubMed: 22895550]
5. Simons FER; Ardusso LRF; Bilo MB; El-Gamal YM; Ledford DK; Ring J; Sanchez-Borges M; Senna GE; Sheikh A; Thong BY; Org WA, World Allergy Organization Guidelines for the Assessment and Management of Anaphylaxis. J Allergy Clin Immun 2011, 127 (3).
6. Jorgensen WL, The Many Roles of Computation in Drug Discovery. Science 2004, 303 (5665), 1813–1818. [PubMed: 15031495]
7. Engvall E; Perlmann P, Enzyme-Linked Immunosorbent Assay (ELISA) Quantitative Assay of Immunoglobulin G; Immunochemistry 1971 (8), 871–874. [PubMed: 5135623]
8. Johnsson B; Lofas S; Lindquist G, Immobilization of Proteins to a Carboxymethyldextran-Modified Gold Surface for Biospecific Interaction Analysis in Surface-Plasmon Resonance Sensors. Anal Biochem 1991, 198 (2), 268–277. [PubMed: 1724720]
9. Sapsford KE; Berti L; Medintz IL, Materials for Fluorescence Resonance Energy Transfer Analysis: Beyond Traditional Donor-acceptor Combinations. Angew Chem Int Edit 2006, 45 (28), 4562–4588.
10. Niesen FH; Berglund H; Vedadi M, The Use of Differential Scanning Fluorimetry to Detect Ligand Interactions that Promote Protein Stability. Nat Protoc 2007, 2 (9), 2212–2221. [PubMed: 17853878]
11. Zhang TT; Wei T; Han YY; Ma H; Samieegohar M; Chen PW; Lian IA; Lo YH, Protein-Ligand Interaction Detection with a Novel Method of Transient Induced Molecular Electronic Spectroscopy (TIMES): Experimental and Theoretical Studies. Acs Central Sci 2016, 2 (11), 834–842.
12. Hergenrother PJ; Depew KM; Schreiber SL, Small-Molecule Microarrays: Covalent Attachment and Screening of Alcohol-containing Small Molecules on Glass Slides. J Am Chem Soc 2000, 122 (32), 7849–7850.
13. Khan M; Park SY, Liquid Crystal-Based Proton Sensitive Glucose Biosensor. Anal Chem 2014, 86 (3), 1493–1501. [PubMed: 24432733]
14. Kim J; Khan M; Park SY, Glucose Sensor using Liquid-Crystal Droplets Made by Microfluidics. Acs Appl Mater Inter 2013, 5 (24), 13135–13139.
15. Yang SY; Wu C; Tan H; Wu Y; Liao SZ; Wu ZY; Shen GL; Yu RQ, Label-Free Liquid Crystal Biosensor Based on Specific Oligonucleotide Probes for Heavy Metal Ions. Anal Chem 2013, 85 (1), 14–18. [PubMed: 23214408]

16. Hu QZ; Jang CH, Liquid Crystal-based Sensors for the Detection of Heavy Metals using Surface-immobilized Urease. Colloid Surface B 2011, 88 (2), 622–626.
17. Popov P; Mann EK; Jakli A, Thermotropic Liquid Crystal Films for Biosensors and Beyond. J Mater Chem B 2017, 5 (26), 5061–5078. [PubMed: 32264091]
18. Lin IH; Miller DS; Bertics PJ; Murphy CJ; de Pablo JJ; Abbott NL, Endotoxin-Induced Structural Transformations in Liquid Crystalline Droplets. Science 2011, 332 (6035), 1297–1300. [PubMed: 21596951]
19. Brake JM; Daschner MK; Luk YY; Abbott NL, Biomolecular Interactions at Phospholipid-decorated Surfaces of Liquid Crystals. Science 2003, 302 (5653), 2094–2097. [PubMed: 14684814]
20. Hartono D; Qin WJ; Yang KL; Yung LYL, Imaging the Disruption of Phospholipid Monolayer by Protein-coated Nanoparticles using Ordering Transitions of Liquid Crystals. Biomaterials 2009, 30 (5), 843–849. [PubMed: 19027155]
21. Gupta VK; Skaife JJ; Dubrovsky TB; Abbott NL, Optical Amplification of Ligand-receptor Binding using Liquid Crystals. Science 1998, 279 (5359), 2077–2080. [PubMed: 9516101]
22. Lai SL; Tan WL; Yang KL, Detection of DNA Targets Hybridized to Solid Surfaces Using Optical Images of Liquid Crystals. Acs Appl Mater Inter 2011, 3 (9), 3389–3395.
23. Chen CH; Yang KL, Detection and Quantification of DNA Adsorbed on Solid Surfaces by using Liquid Crystals. Langmuir 2010, 26 (3), 1427–1430. [PubMed: 19961190]
24. Yang Z; Gupta JK; Kishimoto K; Shoji Y; Kato T; Abbott NL, Design of Biomolecular Interfaces using Liquid Crystals Containing Oligomeric Ethylene Glycol. Advanced Functional Materials 2010, 20 (13), 2098–2106. [PubMed: 22199989]
25. Hartono D; Xue CY; Yang KL; Yung LYL, Decorating Liquid Crystal Surfaces with Proteins for Real-Time Detection of Specific Protein-Protein Binding. Adv Funct Mater 2009, 19 (22), 3574–3579.
26. Ma CD; Adamiak L; Miller DS; Wang XG; Gianneschi NC; Abbott NL, Liquid Crystal Interfaces Programmed with Enzyme-Responsive Polymers and Surfactants. Small 2015, 11 (43), 5747–5751. [PubMed: 26418129]
27. Bi XY; Hartono D; Yang KL, Real-Time Liquid Crystal pH Sensor for Monitoring Enzymatic Activities of Penicillinase. Adv Funct Mater 2009, 19 (23), 3760–3765.
28. Price AD; Schwartz DK, DNA Hybridization-induced Reorientation of Liquid Crystal Anchoring at the Nematic Liquid Crystal/Aqueous Interface. J Am Chem Soc 2008, 130 (26), 8188–8194. [PubMed: 18528984]
29. Macri KM; Noonan PS; Schwartz DK, Receptor-Mediated Liposome Fusion Kinetics at Aqueous/Liquid Crystal Interfaces. ACS Appl Mater Interfaces 2015, 7 (36), 20400–20409. [PubMed: 26317496]
30. Lockwood NA; Mohr JC; Ji L; Murphy CJ; Palecek SR; de Pablo JJ; Abbott NL, Thermotropic Liquid Crystals as Substrates for Imaging the Reorganization of Matrigel by Human Embryonic Stem Cells. Adv Funct Mater 2006, 16 (5), 618–624.
31. Sivakumar S; Wark KL; Gupta JK; Abbott NL; Caruso F, Liquid Crystal Emulsions as the Basis of Biological Sensors for the Optical Detection of Bacteria and Viruses. Adv Funct Mater 2009, 19 (14), 2260–2265.
32. Lockwood NA; de Pablo JJ; Abbott NL, Influence of Surfactant Tail Branching and Organization on the Orientation of Liquid Crystals at Aqueous-Liquid Crystal Interfaces. Langmuir 2005, 21 (15), 6805–6814. [PubMed: 16008390]
33. Yang L; Khan M; Park SY, Liquid Crystal Droplets Functionalized with Charged Surfactant and Polyelectrolyte for Non-specific Protein Detection. Rsc Adv 2015, 5 (118), 97264–97271.
34. Brake JM; Mezera AD; Abbott NL, Effect of Surfactant Structure on the Orientation of Liquid Crystals at Aqueous-Liquid Crystal Interfaces. Langmuir 2003, 19 (16), 6436–6442.
35. Miller DS; Wang XG; Abbott NL, Design of Functional Materials Based on Liquid Crystalline Droplets. Chem Mater 2014, 26 (1), 496–506. [PubMed: 24882944]
36. Bukusoglu E; Pantoja MB; Mushenheim PC; Wang XG; Abbott NL, Design of Responsive and Active (Soft) Materials Using Liquid Crystals. Annu Rev Chem Biomol 2016, 7, 163–196.

37. Lowe AM; Abbott NL, Liquid Crystalline Materials for Biological Applications. Chem Mater 2012, 24 (5), 746–758. [PubMed: 22563142]
38. Carlton RJ; Hunter JT; Miller DS; Abbasi R; Mushenheim PC; Tan LN; Abbott NL, Chemical and Biological Sensing using Liquid Crystals. Liq Cryst Rev 2013, 1 (1), 29–51.
39. Daschner De Tercero M; Abbott NL, Ordering Transitions in Liquid Crystals Permit Imaging of Spatial and Temporal Patterns Formed by Proteins Penetrating into Lipid-Laden Interfaces. Chemical Engineering Communications 2009, 196 (1–2), 234–251.
40. Brake JM; Abbott NL, Coupling of the Orientations of Thermotropic Liquid Crystals to Protein Binding Events at Lipid-decorated Interfaces. Langmuir 2007, 23 (16), 8497–8507. [PubMed: 17595119]
41. Lockwood NA; Gupta JK; Abbott NL, Self-assembly of Amphiphiles, Polymers and Proteins at Interfaces Between Thermotropic Liquid Crystals and Aqueous Phases. Surf Sci Rep 2008, 63 (6), 255–293.
42. Zhao DY; Peng Y; Xu LH; Zhou W; Wang Q; Guo L, Liquid-Crystal Biosensor Based on Nickel-Nanosphere-Induced Homeotropic Alignment for the Amplified Detection of Thrombin. Acs Appl Mater Inter 2015, 7 (42), 23418–23422.
43. Kim HJ; Rim J; Jang CH, Liquid-Crystal-Based Immunosensor for Diagnosis of Tuberculosis in Clinical Specimens. Acs Appl Mater Inter 2017, 9 (25), 21209–21215.
44. Wang X; Yang P; Mondiot F; Li Y; Miller DS; Chen Z; Abbott NL, Interfacial Ordering of Thermotropic Liquid Crystals Triggered by the Secondary Structures of Oligopeptides. Chem Commun (Camb) 2015, 51 (94), 16844–16847. [PubMed: 26440114]
45. Gao JJ; Liu XC; Secinti H; Jiang ZW; Munkhbat O; Xu YS; Guo XH; Thayumanavan S, Photoactivation of Ligands for Extrinsically and Intrinsically Triggered Disassembly of Amphiphilic Nanoassemblies. Chem-Eur J 2018, 24 (8), 1789–1794. [PubMed: 29314349]
46. Kim YK; Raghupathi KR; Pendery JS; Khomein P; Sridhar U; Pablo JJ; Thayumanavan S; Abbott NL, Oligomers as Triggers for Responsive Liquid Crystals. Langmuir 2018, 34 (34), 10092–10101. [PubMed: 30064213]
47. Kamper SG; Porter-Peden L; Blankespoor R; Sinniah K; Zhou DJ; Abell C; Rayment T, Investigating the Specific Interactions Between Carbonic Anhydrase and a Sulfonamide Inhibitor by Single-molecule Force Spectroscopy. Langmuir 2007, 23 (25), 12561–12565. [PubMed: 17973506]
48. Elbaum D; Nair SK; Patchan MW; Thompson RB; Christianson DW, Structure-based Design of a Sulfonamide Probe for Fluorescence Anisotropy Detection of Zinc with a Carbonic Anhydrase-based Biosensor. J Am Chem Soc 1996, 118 (35), 8381–8387.
49. Wang F; Klaikherd A; Thayumanavan S, Temperature Sensitivity Trends and Multi-Stimuli Sensitive Behavior in Amphiphilic Oligomers. J Am Chem Soc 2011, 133 (34), 13496–13503. [PubMed: 21739959]
50. Raghupathi KR; Sridhar U; Byrne K; Raghupathi K; Thayumanavan S, Influence of Backbone Conformational Rigidity in Temperature-Sensitive Amphiphilic Supramolecular Assemblies. J Am Chem Soc 2015, 137 (16), 5308–5311. [PubMed: 25893806]
51. Musevic I; Skarabot M; Tkalec U; Ravnik M; Zumer S, Two-dimensional Nematic Colloidal Crystals Self-assembled by Topological Defects. Science 2006, 313 (5789), 954–958. [PubMed: 16917058]
52. Li LY; Chen SF; Zheng J; Ratner BD; Jiang SY, Protein Adsorption on Oligo(ethylene glycol)-terminated Alkanethiolate Self-assembled Monolayers: The Molecular Basis for Nonfouling Behavior. J Phys Chem B 2005, 109 (7), 2934–2941. [PubMed: 16851306]
53. Herrwerth S; Eck W; Reinhardt S; Grunze M, Factors that Determine the Protein Resistance of Oligoether Self-assembled Monolayers - Internal Hydrophilicity, Terminal Hydrophilicity, and Lateral Packing Density. J Am Chem Soc 2003, 125 (31), 9359–9366. [PubMed: 12889964]
54. Palegrosdemange C; Simon ES; Prime KL; Whitesides GM, Formation of Self-Assembled Monolayers by Chemisorption of Derivatives of Oligo(Ethylene Glycol) of Structure Hs(Ch2)11(Och2ch2)Meta-Oh on Gold. J Am Chem Soc 1991, 113 (1), 12–20.
55. Xu YX; Wang GT; Zhao X; Jiang XK; Li ZT, Self-Assembly of Vesicles from Amphiphilic Aromatic Amide-Based Oligomers. Langmuir 2009, 25 (5), 2684–2688. [PubMed: 19437750]

56. Pani I; Sharma D; Pal SK, Liquid Crystals as Sensitive Reporters of Lipid-Protein Interactions. General Chemistry 2018, 4 (2), 180012.
57. Das D; Sidiq S; Pal SK, A Simple Quantitative Method to Study Protein-Lipopolysaccharide Interactions by Using Liquid Crystals. Chemphyschem 2015, 16 (4), 753–760. [PubMed: 25572441]
58. Alterio V; Di Fiore A; D'Ambrosio K; Supuran CT; De Simone G, Multiple Binding Modes of Inhibitors to Carbonic Anhydrases: How to Design Specific Drugs Targeting 15 Different Isoforms? Chem Rev 2012, 112 (8), 4421–4468. [PubMed: 22607219]
59. Krishnamurthy VM; Kaufman GK; Urbach AR; Gitlin I; Gudiksen KL; Weibel DB; Whitesides GM, Carbonic Anhydrase as a Model for Biophysical and Physical-organic Studies of Proteins and Protein-ligand Binding. Chem Rev 2008, 108 (3), 946–1051. [PubMed: 18335973]
60. Taylor PW; King RW; Burgen ASV, Kinetics of Complex Formation between Human Carbonic Anhydrases an Aromatic Sulfonamides. Biochemistry-Us 1970, 9 (13), 2638–2645.
61. Matulis D; Kranz JK; Salemme FR; Todd MJ, Thermodynamic Stability of Carbonic Anhydrase: Measurements of Binding Affinity and Stoichiometry using ThermoFluor. Biochemistry-Us 2005, 44 (13), 5258–5266.
62. Meister K; Roeters SJ; Paananen A; Woutersen S; Versluis J; Szilvay GR; Bakker HJ, Observation of pH-Induced Protein Reorientation at the Water Surface. J Phys Chem Lett 2017, 8 (8), 1772–1776. [PubMed: 28345915]
63. Roy R; Sandanaraj BS; Klaikherd A; Thayumanavan S, Tuning Substrate Selectivity of a Cationic Enzyme using Cationic Polymers. Langmuir 2006, 22 (18), 7695–7700. [PubMed: 16922552]
64. Tilton RD; Robertson CR; Gast AP, Manipulation of Hydrophobic Interactions in Protein Adsorption. Langmuir 1991, 7 (11), 2710–2718.
65. Wertz CF; Santore MM, Effect of Surface Hydrophobicity on Adsorption and Relaxation Kinetics of Albumin and Fibrinogen: Single-Species and Competitive Behavior. Langmuir 2001, 17 (10), 3006–3016.
66. Phan HTM; Bartelt-Hunt S; Rodenhausen KB; Schubert M; Bartz JC, Investigation of Bovine Serum Albumin (BSA) Attachment onto Self-Assembled Monolayers (SAMs) Using Combinatorial Quartz Crystal Microbalance with Dissipation (QCM-D) and Spectroscopic Ellipsometry (SE). Plos One 2015, 10 (10).
67. Malmsten M, Formation of Adsorbed Protein Layers. J Colloid Interf Sci 1998, 207 (2), 186–199.
68. Rich RL; Quinn JG; Morton T; Stepp JD; Myszka DG, Biosensor-based Fragment Screening using FastStep Injections. Anal Biochem 2010, 407 (2), 270–277. [PubMed: 20800052]
69. van den Burg B; Eijsink V, Thermolysin and Related Bacillus Metallopeptidases Handbook of Proteolytic Enzymes, Vols 1 and 2, 3rd Edition 2013, 540–553.
70. Bewley TA, A Novel Procedure for Determining Protein Concentrations from Absorption-Spectra of Enzyme Digests. Anal Biochem 1982, 123 (1), 55–65. [PubMed: 7114476]

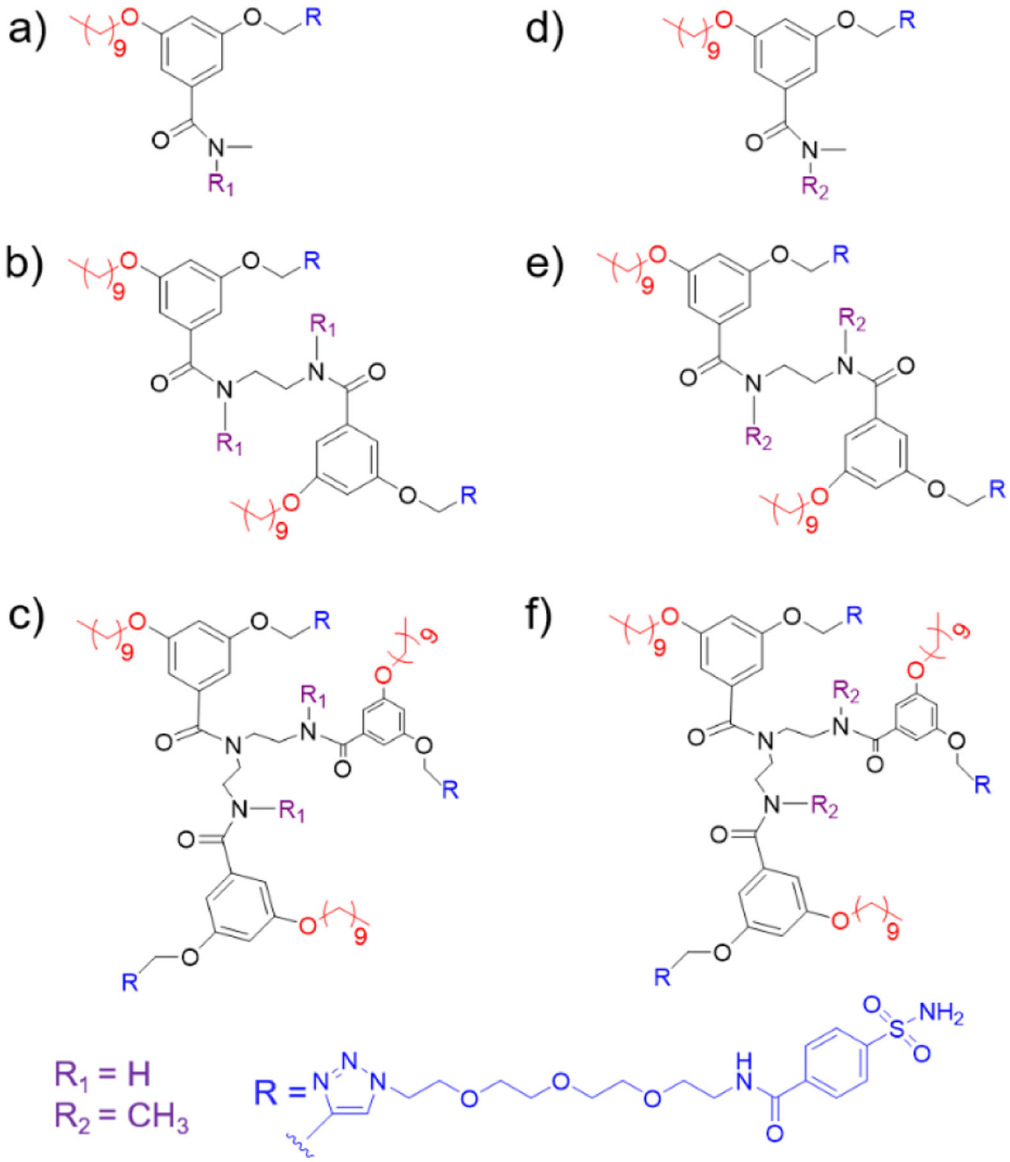

Figure 1.

Molecular structures of amphiphilic oligomers examined in this study: (a) ***H***-monomer, (b) ***H***-dimer, (c) ***H***-trimer, (d) ***CH$_3$***-monomer, (e) ***CH$_3$***-dimer, (f) ***CH$_3$***-trimer.

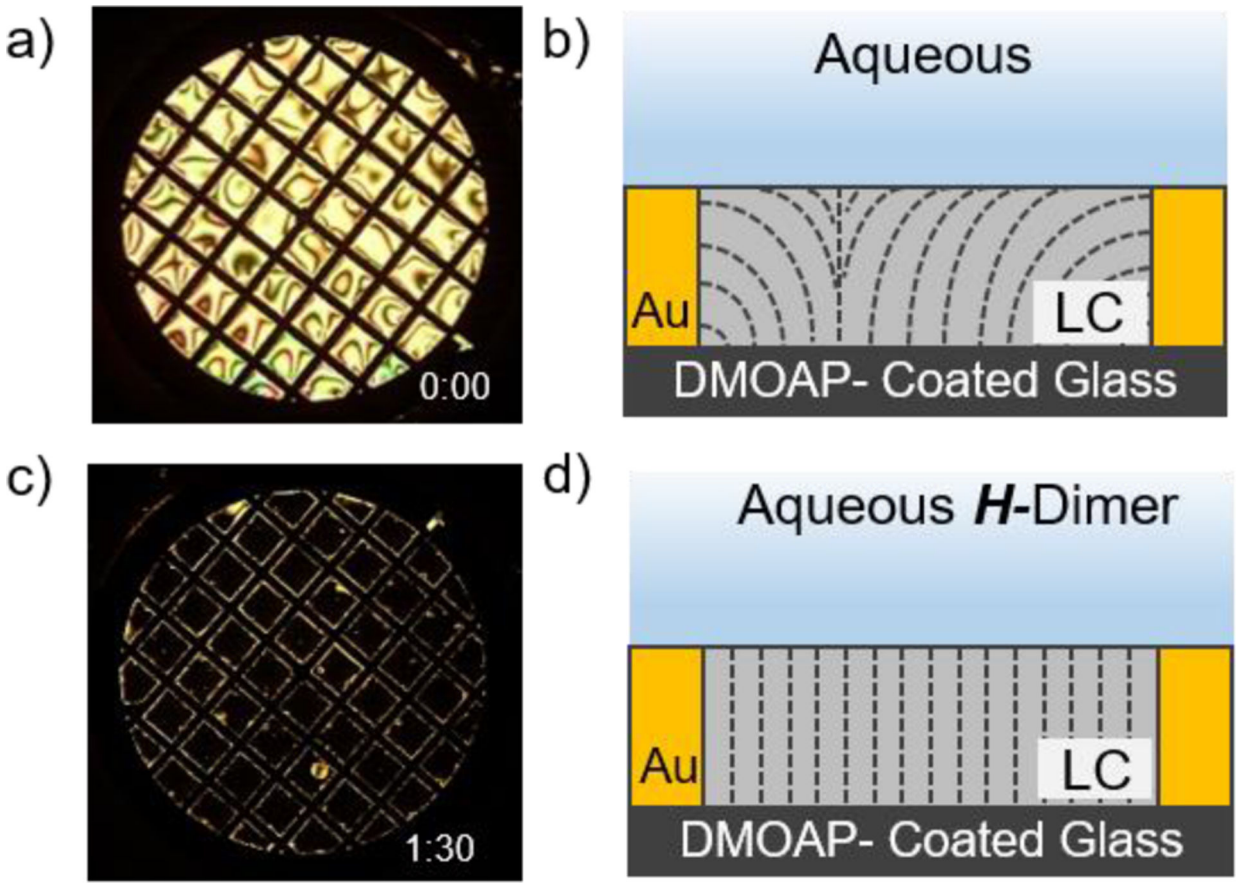

Figure 2.

(a,c) Optical micrographs (crossed-polarizers) and (b,d) schematic illustrations of aqueous-LC interfaces with (b) planar anchoring and (d) homeotropic anchoring upon incubation against 20 μM ***H***-dimer. All samples were prepared with PBS.

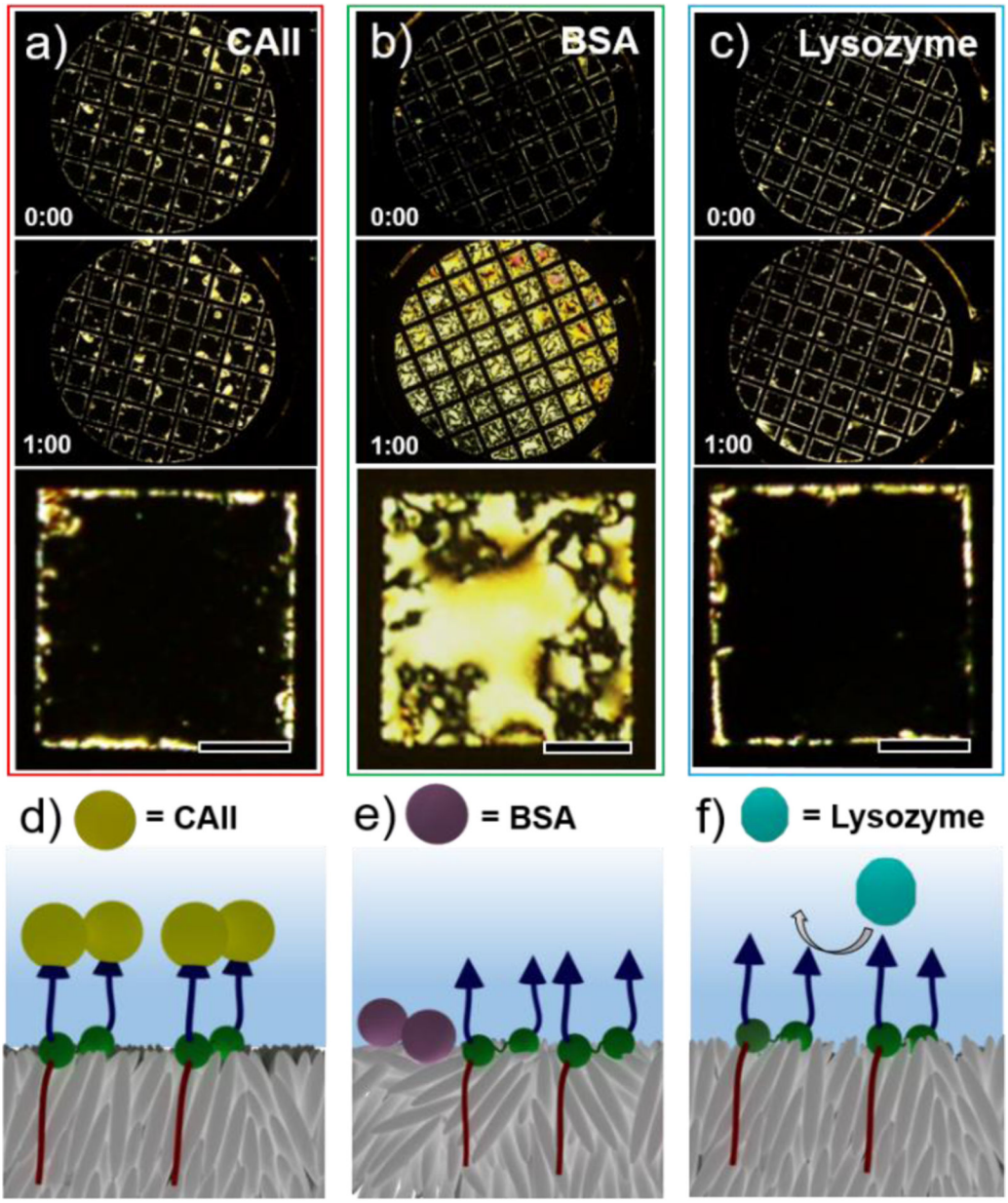

Figure 3.

(a-c) Optical micrographs (crossed-polarizers) and (d-f) corresponding schematic illustrations of the responses of aqueous-LC interfaces decorated with the ***H***-dimer (20 μM) to (a,d) CAII (0.4 μM), (b,e) BSA (4 μM), and (c,f) lysozyme (4 μM). Third row in (a-c) shows magnified images of second row (1 hour after the incubation of LC films). Scale bar is 100 μm.

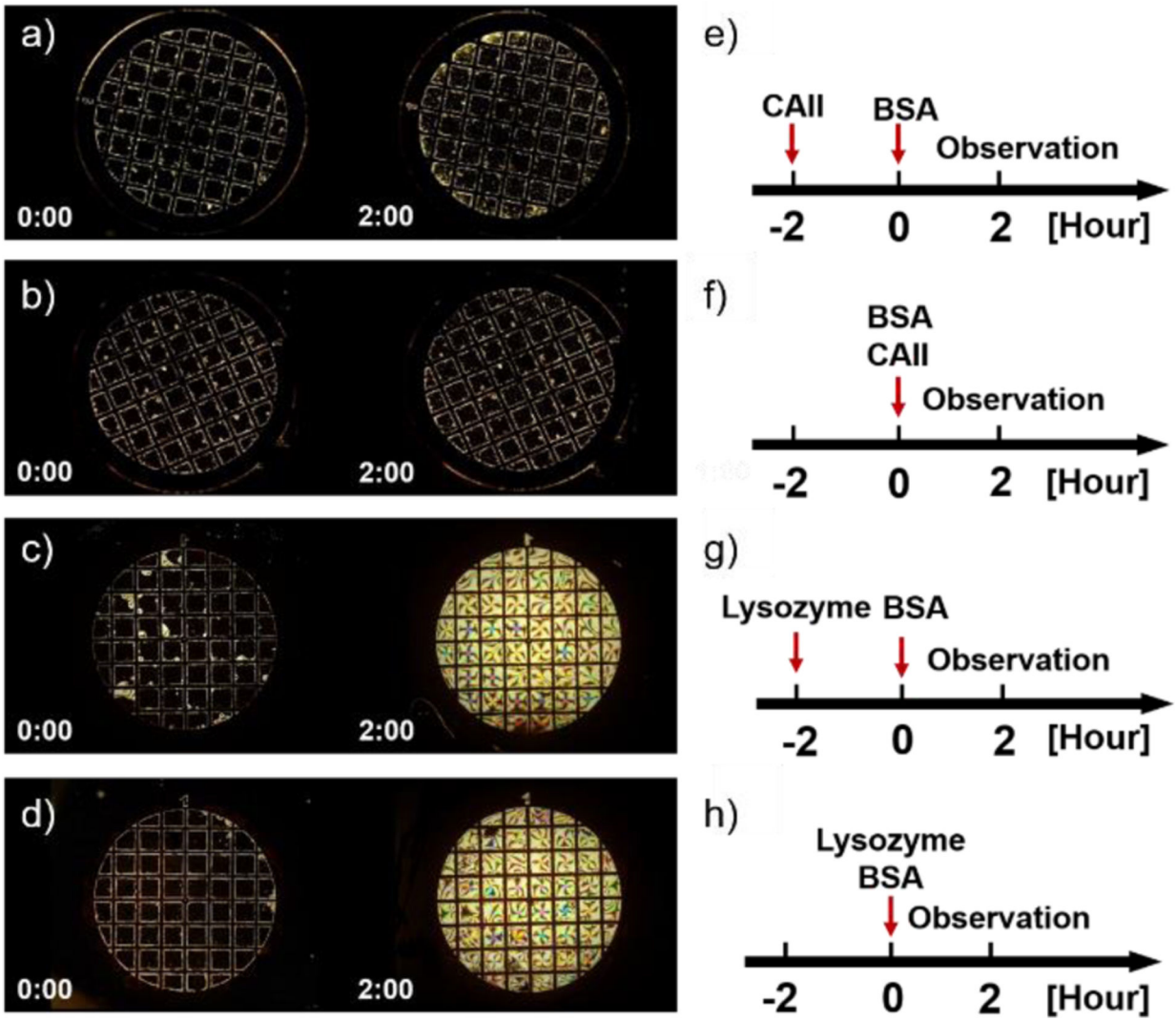

Figure 4.

(a-d) Optical micrographs (crossed-polarizers) of anchoring transitions at aqueous-LC interfaces decorated with ***H***-dimer (20 μM) that are triggered by (a) BSA (1 μM) after incubating first against CAII (0.4 μM), (b) CAII (0.4 μM) and BSA (1 μM) added simultaneously, and (c) BSA (1 μM) after incubating against lysozyme (1 μM), (d) lysozyme (1 μM) and BSA (1 μM) added simultaneously. (e-h) Corresponding timelines for the sample observation and the addition of CAII (0.4 μM), BSA (1 μM), and lysozyme (1 μM) into the aqueous solutions. All samples were incubated for 2 hours prior to observation.

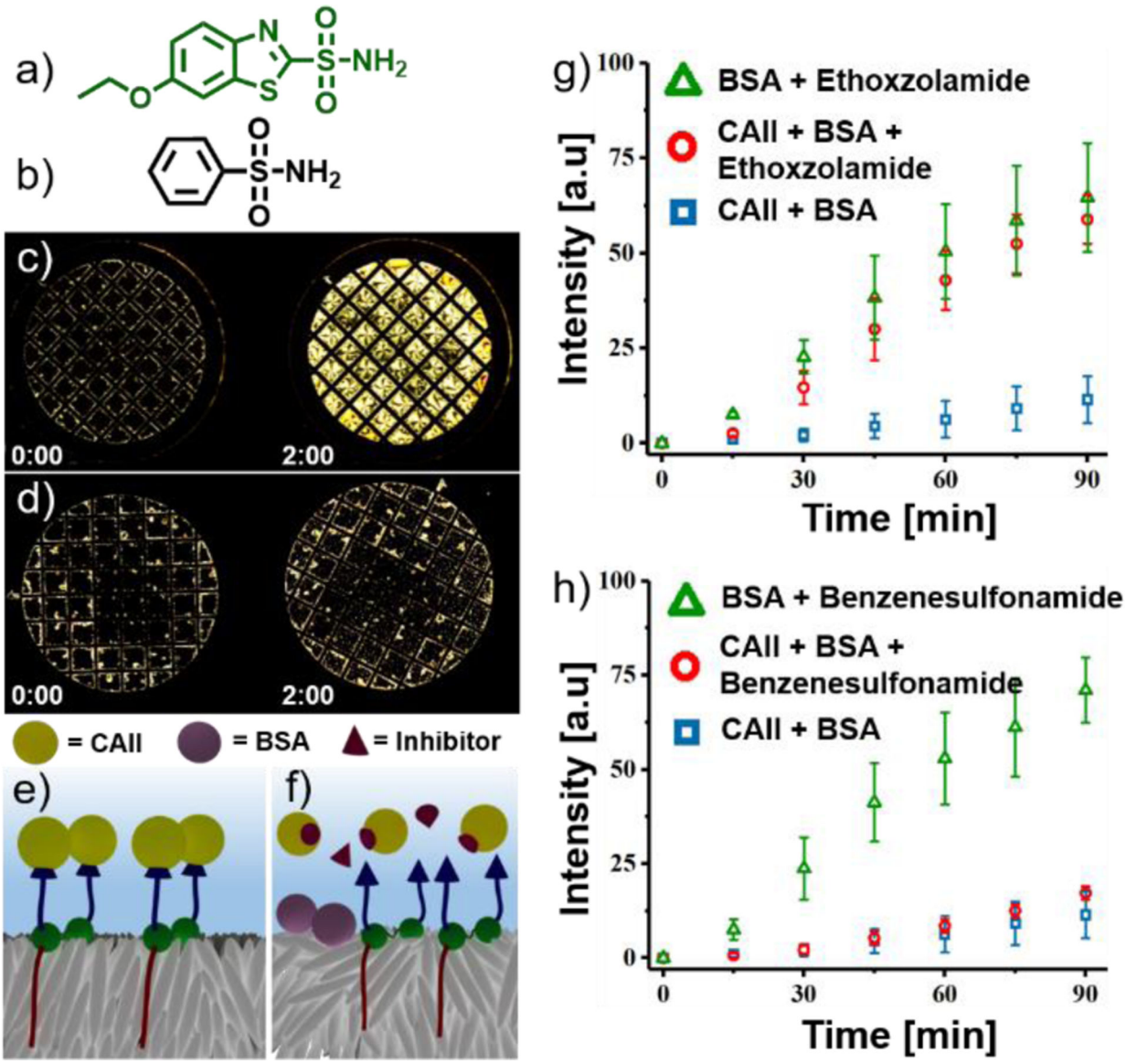

Figure 5.

(a,b) Molecular structures of inhibitors (a) ethoxzolamide and (b) benzenesulfonamide. (c,d) Optical micrographs (crossed-polarizers) of the ***H***-dimer-CAII-decorated interface of the LC after incubation in c) 0.4 μM CAII + 1 μM BSA + 4 μM ethoxzolamide and d) 0.4 μM CAII + 1 μM BSA + 4 μM benzenesulfonamide. (e, f) Schematic illustrations of LC response to dimer and CAII e) without inhibitor depicting homeotropic LC anchoring and f) with inhibitor, depicting tilted LC anchoring. (g,h) Time-dependent change in intensities of light transmitted through the LC films following incubation with (g) ethoxzolamide and (h) benzenesulfonamide. Quantification of intensity of images was performed with NIH ImageJ software. The concentration of both inhibitors was 4 μM and the concentration of BSA in all cases was 1 μM. Mean ± s.d. (n = 3).

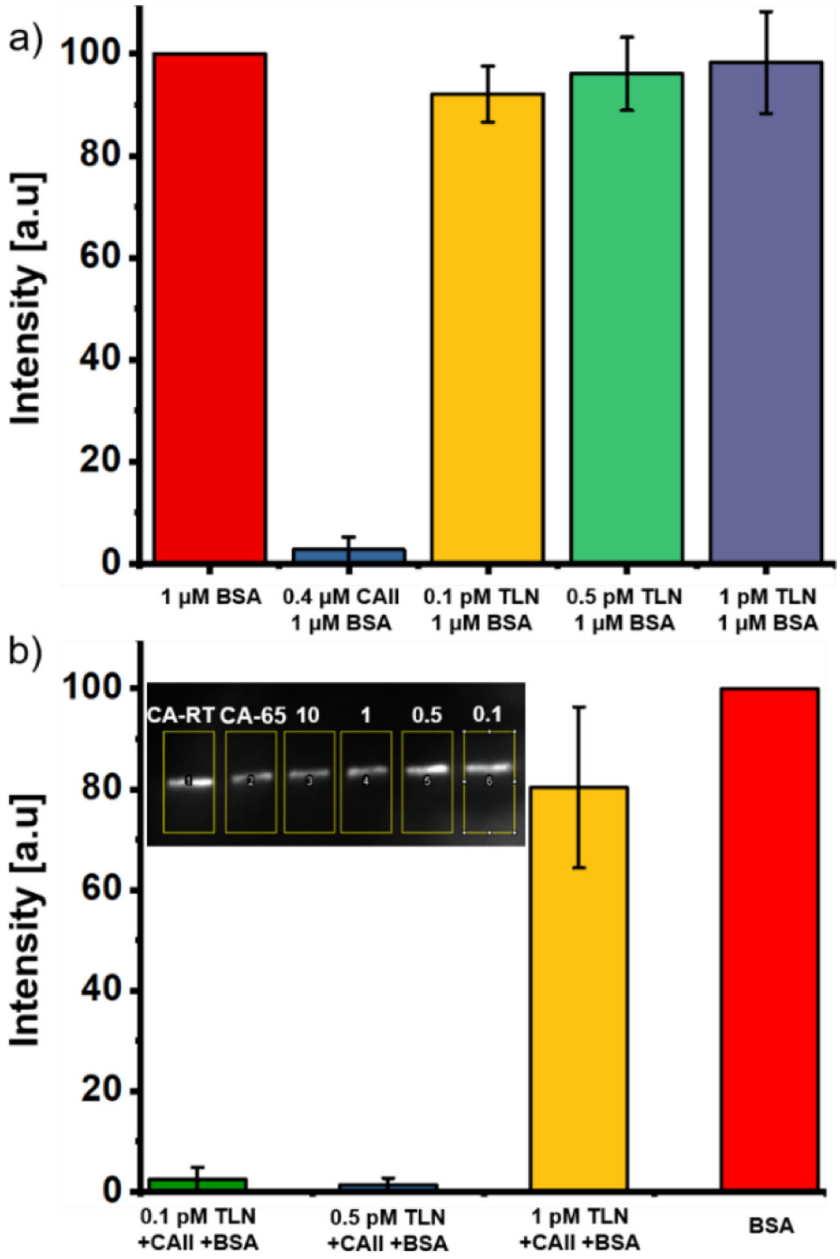

Figure 6.

(a) Optical response of the aqueous-LC interface of all control samples. (b) Relative intensity of light transmitted through the aqueous-LC interface (crossed-polarizers) as a function of concentration of TLN. Inset shows western blot analysis of CAII degradation following incubation with 10, 1, 0.5, 0.1, 0 pM thermolysin for 1 hour. Quantification of intensity of images was performed with NIH ImageJ software. Mean ± s.d. (n = 4)

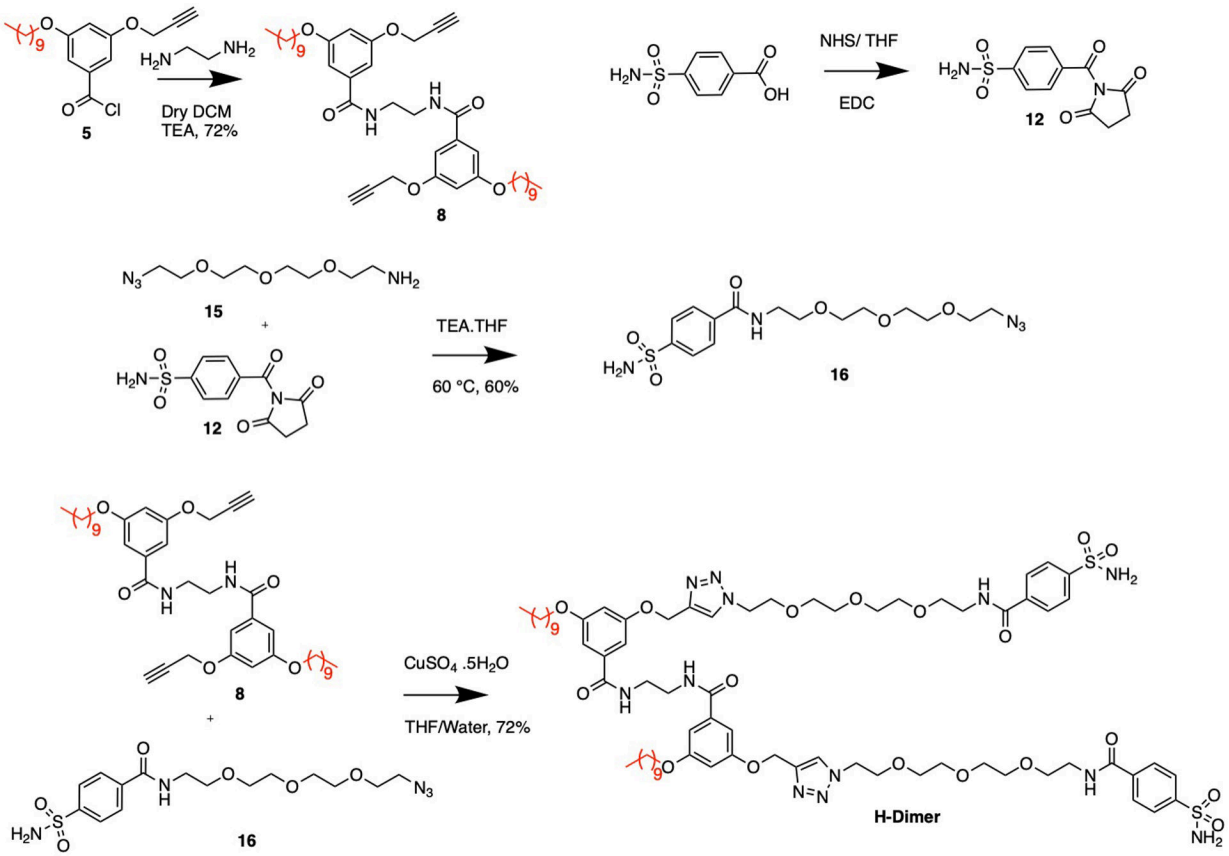

Scheme 1:
Synthetic pathway for ***H***-dimer.

Table 1.

Properties of Proteins Used in This Study

	CAII	**BSA**	**Lysozyme**
Origin	bovine	bovine	chicken
M.W. [kDa]	29	66	14
pI	5.4	5.3	11.4

Table 2.

Zeta Potential Measurements of Aqueous-LC Interfaces

Sample	**Zeta Potential [mV]***
5CB droplet in water	−70 ± 1
5CB droplet in PBS	−28 ± 3[26]
5CB droplet in 20 μM ***H***-dimer	−40 ± 1[a]

* Mean ± s.d. (n=3)

[a] zeta potential measurement performed in PBS (pH 7.4)

Table 3.

Thermolysin Activity Measurements via Western Blot

Thermolysin Concentration	Normalized Band Intensity*
10	0.42 ± 0.28
1	0.66 ± 0.29
0.5	0.87 ± 0.33
0.1	0.99 ± 0.36

* Mean ± s.d. (n = 4)